A Selection of Oriented Crystal Preparations Useful for Teaching Optical Fundamentals

Daniel Kile

Introduction

I have taught optical mineralogy at both the Colorado School of Mines in Golden, Colorado, and optical crystallography at the Hooke College of Applied Sciences in Chicago, as well as at the U.S. Geological Survey in Denver, for nearly 25 years. This paper describes some of the more interesting preparations I have used in these classes to engage the students, illustrate optical principles, and reinforce learned optical concepts. From a historical perspective, it is surprising how many of these phenomena were known by the early 1800s, using comparatively primitive instruments, notably by J.-B. Biot and David Brewster. In fact, many of the phenomena described below were documented by Brewster in 1835. To accommodate the need for teaching aids, a wide range of mineralogical preparations

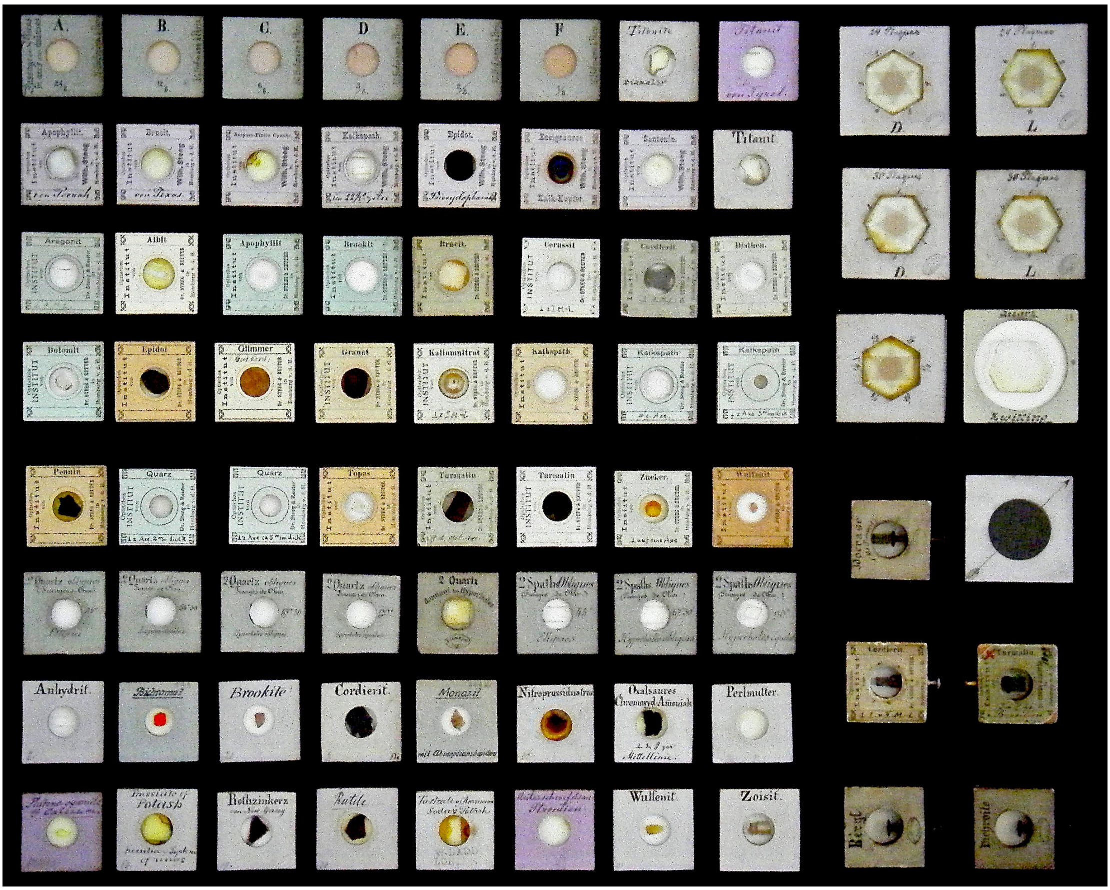

Fig. 1. Cork mounted mineral preparations. Nörrenberg crossed mica sections are in the top row. Preparations in the 2nd row are signed 'Wilhelm Steeg, Homburg', and date back to 1873. Mounts in the 3rd – 6th rows are labeled 'Steeg & Reuter, Homburg'. Preparations in the bottom 2 rows are unlabeled, but most probably by Steeg & Reuter. The larger mounts at top right are crossed mica preparations after Reusch. Rotating crystal mounts are at lower right (see also Fig. 7).

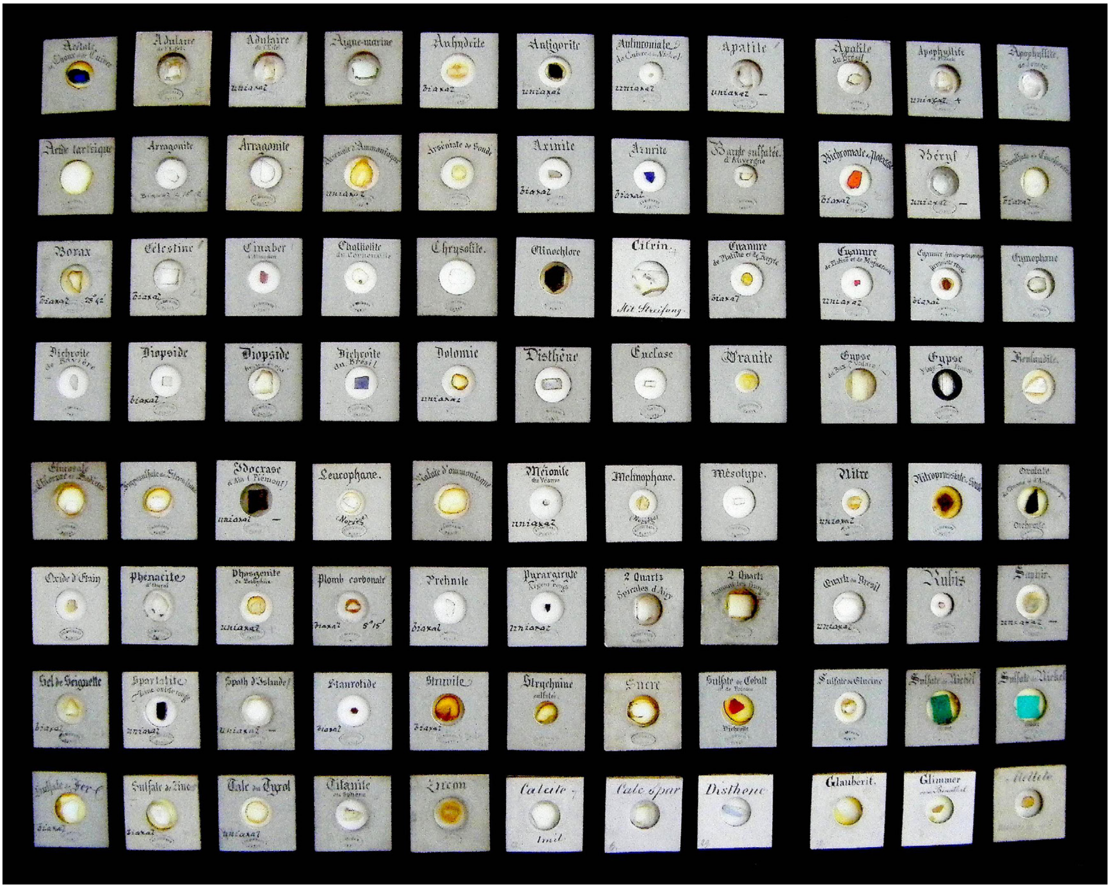

Fig. 2. These preparations are signed 'J.G. Hofmann, Paris', who was most likely a secondary distributor of Steeg & Reuter mounts. They represent a wide range of oriented crystal sections.

were commercially fabricated from the last quarter of the 19th century through the first half of the 20th. Phenomena such as optical character (uniaxial-biaxial), optic sign (positive or negative), birefringence, extinction angle, optic angle (2V), pleochroism, dispersion (e.g., optic axis, crossed axial plane, horizontal and inclined), optical activity, and anomalous interference colors were represented, among others. Crystals for these oriented sections were obtained from numerous worldwide sources; they were carefully selected for suitable optical properties, then meticulously oriented and ground and polished to exacting standards using specialized goniometer apparatus. Synthetic organic or inorganic crystals were often utilized as well, inasmuch as their optical properties were identical to those of naturally occurring minerals. It is assumed that the reader of this article will have a rudimentary knowledge of basic mineralogy and mineral optics, as a comprehensive description of the terms and concepts is well beyond the scope of this paper; a concise summary of basic optical principles is given in Kile (2003) or in any introductory textbook of optical mineralogy (e.g., Nesse, 2013). Delly (2017) provides an extensive treatise on polarised light microscopy. The Appendix below also provides brief definitions of some of the optical terms used herein.

Fig. 3. Cork mounted mineral sections prepared by Wilhelm Steeg prior to 1873 (top row), or later by Steeg & Reuter (2nd row); those in the 3rd and 4th rows are hand-labeled in French with a secondary retailer label of J.G. Hofmann, Paris. The cinnabar ("Cinaber") and titanite were the most expensive preparations sold by the firm.

Mineralogical Preparations and Instruments for Observation

In early years, a majority of the commercial mineralogical preparations designed for teaching and research were manufactured by the Wilhelm Steeg Company, and later by the firm of Steeg & Reuter in Germany (Figs. 1–3). See Kile (2012) and Medenbach and Reimann (2003) for a history of these venerable firms. Up to the Mid-20th century they were mounted in cork frames, ca. 3.5 cm

Fig. 4. A complete set of 50 oriented mineral sections prepared by Steeg & Reuter on glass petrographic slides, ca. 1950s.

square, after which glass slides (ca. 28 x 47 mm, Fig. 4) were utilized for oriented crystal mounts. A number of these preparations were exceptionally elaborate and required extraordinary skill in manufacturing; some were composed of more than one mineral type, or of multiple layers or orientations of a single mineral, while others

Fig. 5. Early Fuess polariscopes: A conoscope (left) and a stauroscope (right), ca. 1900; both were designed to examine cork-mounted preparations. Conoscopes, with highly converging lenses, were used to examine interference figures. The analyser is a Nicol prism, whereas the polarizer consists of a stack of glass plates and a mirror which provide polarised light via reflection. Stauroscopes (a rare form of orthoscope used to determine precise extinction angles) were utilized to examine mineral sections in orthoscopic light.

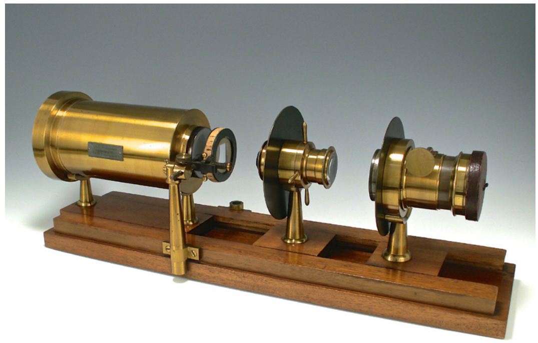

Fig. 6. A bench polariscope, manufactured by Steflitschek, Vienna. This instrument is used to project an image of cork-mounted specimens onto a screen for classroom demonstration.

were elaborately carved gypsum crystal cleavages to show different interference colors. Crystals in many of the early preparations, especially the cork-mounted ones, were cut much thicker than a normal thin section in order to accentuate a given optical property, which would be otherwise be difficult to assess. Accordingly, instruments collectively referred to as polariscopes (which included consocopes for conoscopic studies and orthoscopes for orthoscopic investigations) were designed to investigate the optical properties shown by these early mounts (Fig. 5). These early instruments were made mostly by the Steeg & Reuter Company, or a few other firms such as R. Fuess, and are now scarce and expensive. However, a Leitz Ortholux-I petrographic microscope (ca. 1960s) works very well with these mounts, especially when employing a long working distance condenser top element (a Leitz 0.70/L4 or a 0.60/L11 top lens, depending on the thickness of the mount, threaded to fit a 700 series polarising condenser) that illuminates a full field of view with the objectives focused relatively high above stage level. Most research-grade petrographic microscopes will also suffice. Additionally, a number of early firms manufactured equipment for the screen projection of mineralogical mounts

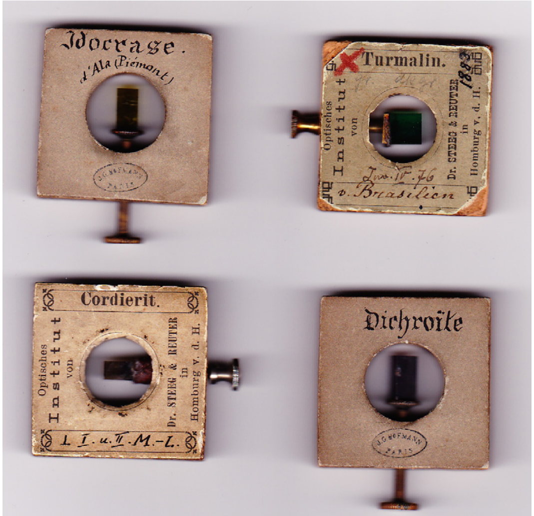

Fig. 7. Rotating crystal mounts prepared by Steeg & Reuter.

in a classroom setting (Fig. 6). These relatively large instruments utilized a glass-plate polariser (i.e. polarisation by reflection) in place of a large calcite prism, which at that time was fearfully expensive, the only source being at Helgustadir, Iceland, which was being rapidly depleted (Kristjansson, 2003).

Optical Phenomena that can be Demonstrated with Oriented Preparations

Pleochroism: Iolite (Cordierite).

Iolite is the trade name for gem-quality cordierite (a magnesium-aluminum silicate), the latter term being the proper mineral name (it was also called "dichroite" in earlier days). Cordierite is a strongly pleochroic (actually, trichroic) mineral, which shows distinctly different colors in different crystal orientations in plane polarised light. Pleochroism in plane polarised light is a result of two mutually perpendicular rays of light passing through the mineral that are absorbed differently, resulting in correspondingly different colors. Minerals with very strong pleochroism (such as cordierite or tourmaline) can show the effect even in white light. Steeg & Reuter manufactured a number of

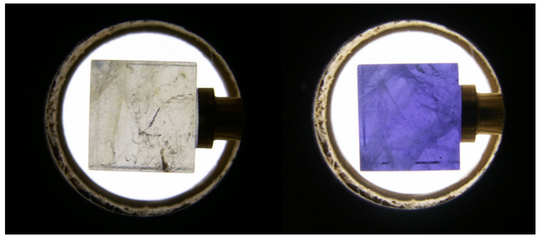

Fig. 8. A cordierite (iolite) rotating crystal in a cork frame, showing distinct pleochroism in white light as the crystal is rotated. This mount is a surrogate prepared by the author for use by students.

rotating crystal prisms mounted in a cork frame to demonstrate this property, examples of which are shown in Fig. 7. The pleochroism of a rotating cordierite cube in white light is illustrated in Fig. 8, and Fig. 9 shows pleochroism in two different orientations of a synthetic organic compound.

Uniaxial Character in 3T Micas: Nörrenberg crossed mica plates.

Phyllosilicates (the mica-group minerals) are

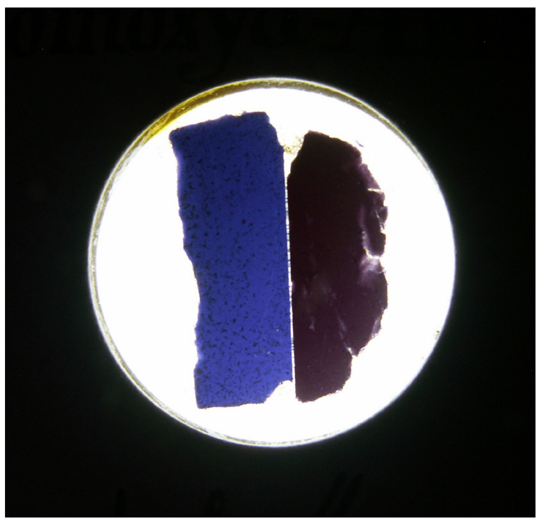

Fig. 9. A Steeg & Reuter cork mount showing two orientations of 'Oxalsaures chromoxyd–Ammoniak', a synthetic compound that shows strong pleochroism in white light in sections perpendicular and parallel to the Bxa. Optical properties for organic and inorganic compounds are identical to those of naturally occurring minerals, hence they constitute excellent demonstration material.

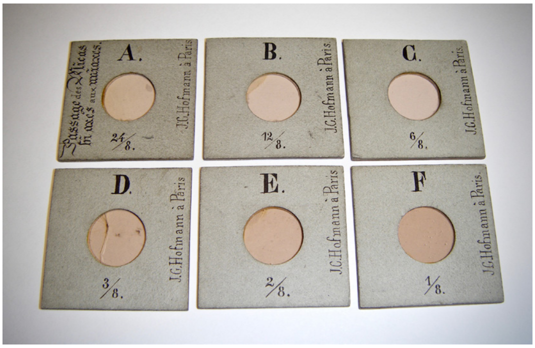

Fig. 10. A set of Nörrenberg crossed micas, composed of from 1 to 24 cleavage plates of micas, crossed at 90º, signed 'J.G. Hofmann / Paris'. Inscribed 'Passage des Micas – bi axes aux uniaxes', they are designed to demonstrate the effect of polytype layer stacking to yield a uniaxial interference figure in a biaxial mineral.

monoclinic (with one inclined crystallographic axis) and usually characterized by perfect cleavage along the (001) plane; the cleavage arises from weak bonding between T-O-T (tetrahedral-octahedral-tetrahedral) layers. Being of monoclinic symmetry, a biaxial interference figure is expected; muscovite (a potassium-aluminum silicate), for example, shows an acute bisectrix (Bxa) figure of about 42º (thus, both optic axes will appear in the conoscopic field of view). However, some micas, notably biotite, show a sensibly uniaxial interference figure that is inconsistent with its monoclinic symmetry. Elaborate preparations, known as "Nörrenberg plates", include six cork mounted mica cleavages (Fig. 10), all but the first consisting of multiple stacked plates, each perfectly oriented at 90º to one another; they were prepared to illustrate how this seeming anomaly of symmetry occurs. The interference figures for a sequence of six stacked plates are shown in Fig. 11.

Mica crystals are composed of stacked monoclinic silicate plates (or sheets); the symmetry of the stacking sequence determines the polytype

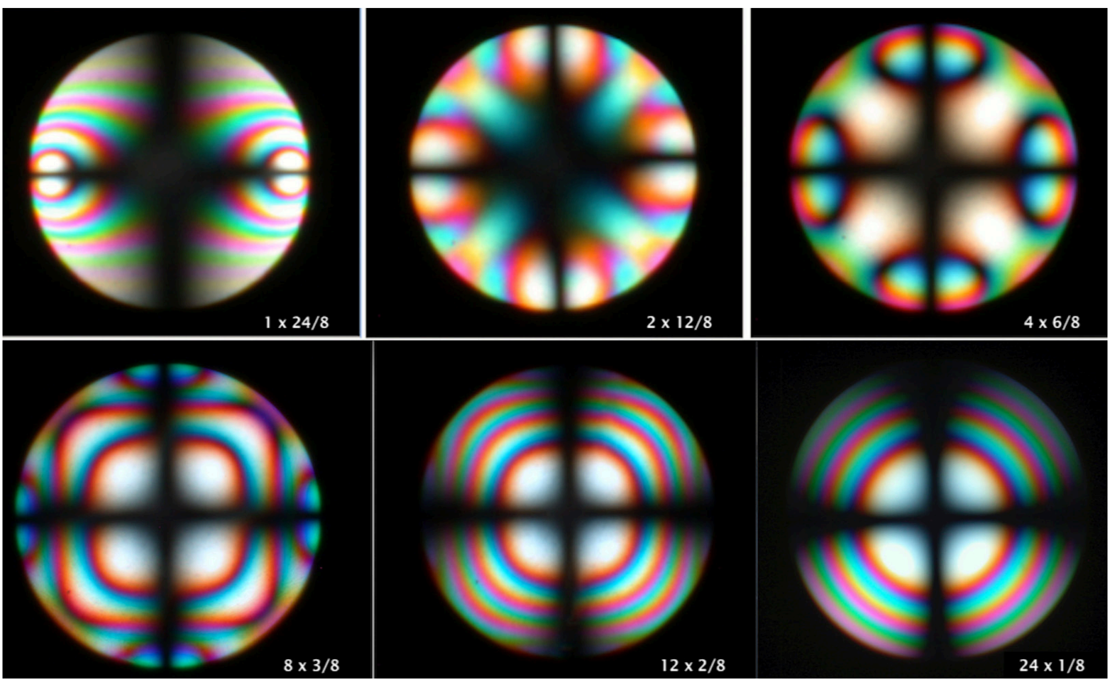

Fig. 11. Nörrenberg interference figures. The series of six interference figures shows the progressive change from a biaxial Bxa figure to a uniaxial cross as mica layers (of decreasing thickness in each mount) are successively stacked. The number of plates in each mount (from 1 to 24) is shown in the lower right of the frame, and the retardation (i.e., thickness of the plates) is given by the fractional number.

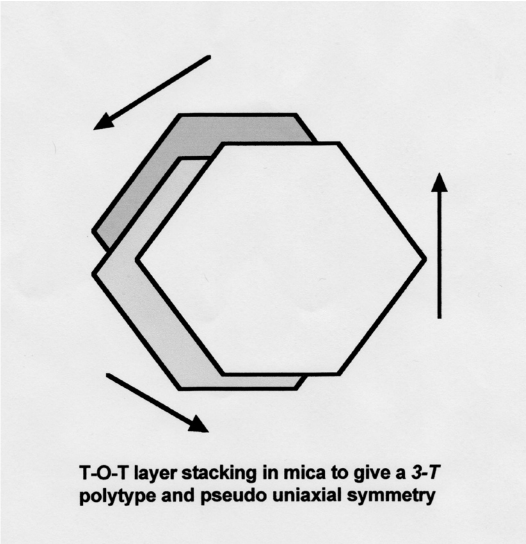

Fig. 12. A mica stacking diagram, showing the sequential and symmetrical stacking of layers of silicate sheets to create a *3T* polytype with a sensibly uniaxial interference figure.

and thus the interference figure. For example, plates stacked sequentially in one direction (i.e., symmetrically, as illustrated in Fig. 12) will give a uniaxial interference figure referred to as a *3T* polytype, whereas asymmetrical stacking (e.g., in an alternating or reciprocating sequence) results in a 1*M*, $2M_1$ or $2M_2$ polytype, with a distinctly biaxial figure. Thus, the symmetrically arranged plates modify the passage of light to approximate a uniaxial symmetry and interference figure. Note, however, that in a *3T* biotite cleavage, there often remains a very slight separation of the central isogyres, indicating a small degree of biaxiality.

Retardation, Birefringence, and Thickness (I): Gypsum Carving.

One of the most important equations in the realm of optical mineralogy, in my opinion, expresses the relation between retardation, birefringence, and mineral thickness. The equation is written as

$$\Delta = t\,(n_2 - n_1) \qquad (1)$$

where Δ represents retardation in nm (the value of which correlates to an interference color,); it is crystal or grain thickness in nm; and n_2, n_1 are maximum and minimum indices of refraction, with $(n_2 - n_1)$ representing birefringence which is also expressed as δ. Measurement of any two of these parameters can give a calculated value of the third. Thus, knowing a crystal thickness and measuring its maximum retardation with a graduated quartz wedge, Berek compensator (e.g., Kile, 2021), or Ehringhaus compensator, etc., can permit calculation of birefringence, a quantitative property that can help identify an unknown mineral.

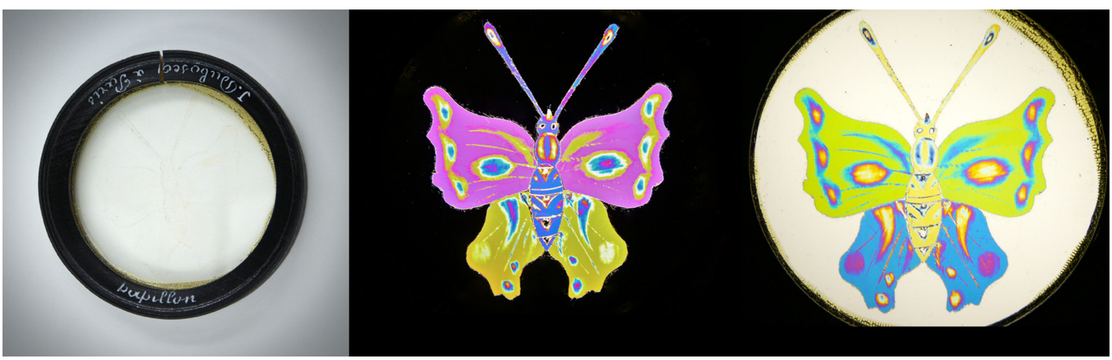

Fig. 13. Left: A butterfly ('papillon') made of carved gypsum in a circular wood frame prepared by the firm of Duboscq in Paris. The faint outline of the butterfly can be seen in white light. Center and right: the same Duboscq butterfly in crossed polarised light (center) and parallel polarised light (right). The skilled workmanship required to fabricate these mounts is impressive, to say the least!

Fig. 14. Duboscq mounts of carved gypsum showing a parrot and a pansy, shown in crossed polarised light.

The selenite variety of gypsum, a hydrous calcium sulfate, is exceedingly soft (Mohs hardness=2) and has perfect cleavage on the (010) crystal face and a birefringence of 0.010. These properties lend it to carving to different thicknesses yielding varying interference colors. Most of these preparations were fabricated by craftsmen at the firm of Steeg & Reuter in Germany, who created a number of motifs, including (but not limited to) scenic landscapes, parrots, butterflies, and flowers (Figs. 13,14). Imaging these preparations between crossed polars yields stunning colors and detail, while viewing between parallel polars yields complimentary interference colors. The extraordinary skill and patience required to perform this task is simply amazing. The sheer beauty of these preparations can captivate a student, which then extends to an inquiry of the relation of crystal retardation, thickness and interference color. The firm of Ernst Leitz provided, with their Prado polarising projection apparatus, a set of 15 glass slides of oriented mineral sections to demonstrate various optical properties; among these was a gypsum cleavage of unequal thickness (Fig. 15), and either a tulip (Fig. 16) or a butterfly.

Retardation, Birefringence, and Thickness (II): Geometric Mica Preparations and Gypsum–Mica Combinations.

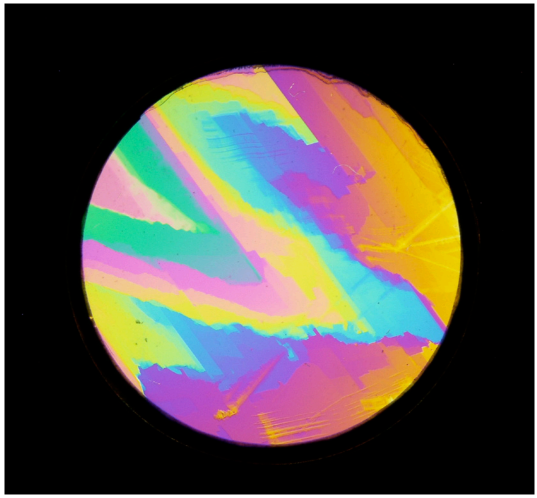

Fig. 15. A cleavage fragment of gypsum parallel to (010), with unequal thickness in crossed polarised light, artistically highlighting the relation between thickness and interference color of the crystal. This glass slide mounted preparation is one of 15 that are included with the Leitz Prado polarising projector from the 1960s.

These, and related combination preparations were painstakingly manufactured largely for artistic merit to engage student interest in optical phenomena, as well as reinforce an understanding of equation (1). The photos shown in Figs. 17 and 18 represent only a very small sample of the wide range of geometric patterns that were fabricated from mica cleavages. Gypsum (selenite) – mica combinations are made of multiple layers of cleavages of these two minerals. In Fig. 19 the mount frames are annotated both with the stacking sequence (e.g., "m s m m s m", where m = mica, and s = selenite) and the individual plate orientation (e.g. "| | – – | |", illustrating a N-S or E-W orientation of the principal vibration direction for a given plate). The thickness and orientation have to be absolutely precise to yield a symmetrical figure. While, admittedly, these preparations do not convey a fundamental optical concept, they definitely impart a memorable image!

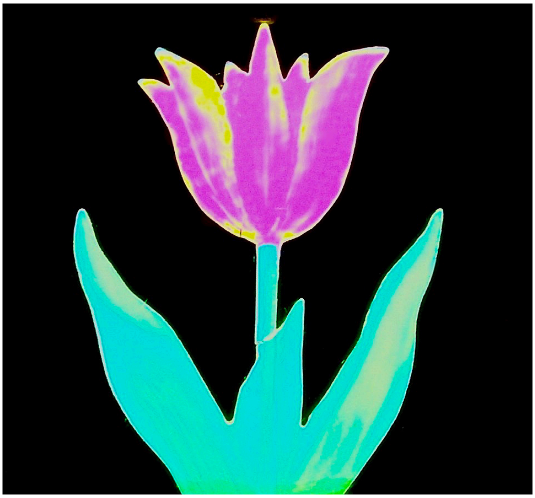

Fig. 16. A carved gypsum cleavage showing a tulip motif in crossed polarised light, from a Prado polarising projector set from the 1960s.

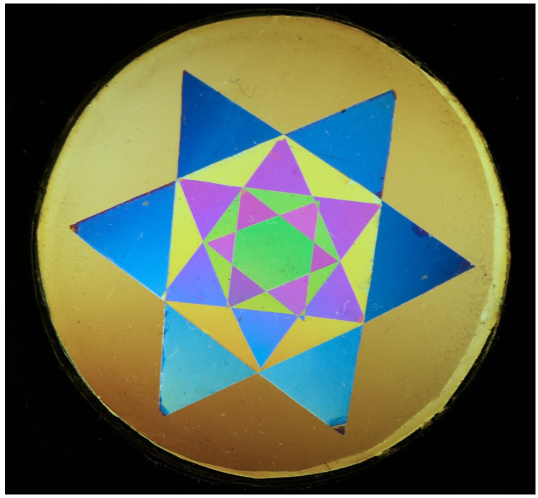

Fig. 18. Geometric micas. Stacked mica cleavage plates were also manufactured to produce a wide variety of geometric shapes to illustrate the fundamental optical relation of retardation vs. thickness.

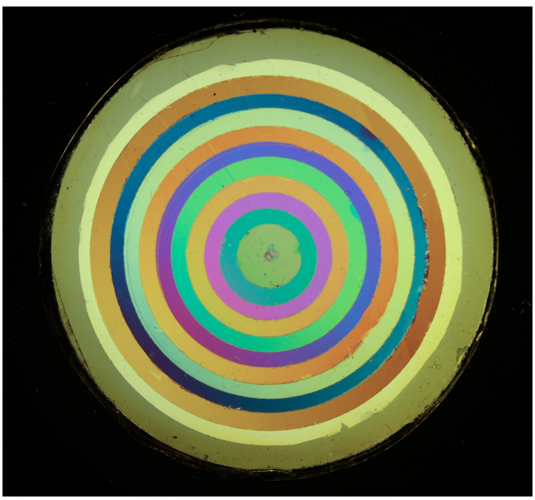

Fig. 17. Stacked circular micas. A concentric stack of circular, oriented sections of mica plates, with decreasing diameter with each added section, gives an impressive rendition of a color wheel, another example illustrating the relation of thickness and retardation. Note that the interference colors increase with increasing thickness (i.e., birefringence) toward the center of the circle.

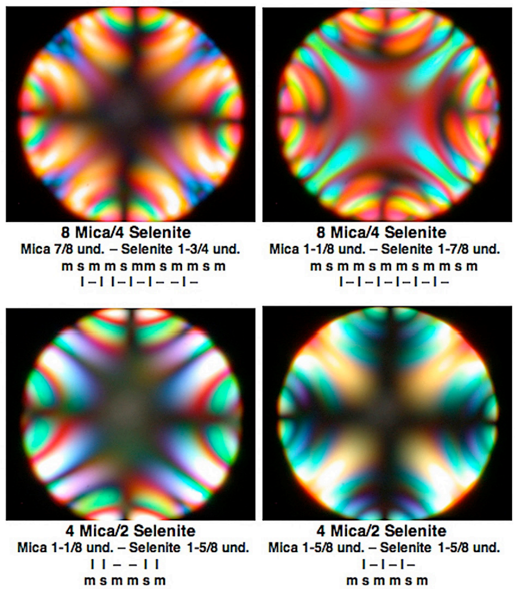

Fig. 19. Mica-gypsum combinations. Stacks of alternating layers of mica and gypsum cleavage sections create exceptional interference figures.

Fig. 20. A natural crystal of cerussite, 4 cm; from Tsumeb, Namibia.

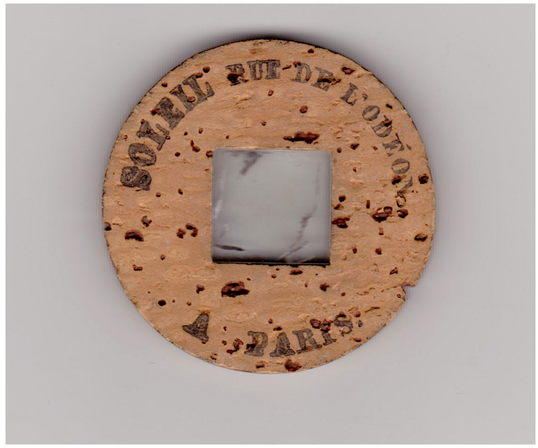

Fig. 21. A Soleil, Paris cork mount of 'plomb carbonate', manufactured ca. 1854 (!)

Optic Axis Dispersion: Cerussite, Cavansite and Pentagonite.

Dispersion of white light in interference figures was known since the early 1800s; it is a fundamental optical property of light that relates to different indices of refraction (or velocities) for different wavelengths, which can be diagnostic in mineral identification. Cerussite, a lead carbonate, (Figs. 20 and 21) is a mineral that shows prominent optic axis dispersion. An optic axis is a point of zero retardation, where light travels along an isotropic direction through a given crystal. In a biaxial mineral, with two optic axes, the emergence of an optic axis (melatope) in a conoscopic interference figure is an area of darkness *in white light*, around which the isogyres rotate when the stage is rotated. The separation between the two optic axes (or melatopes) is defined as the optic angle, or 2V, and is specific to a given wavelength. If, however, the optic angle varies appreciably for different wavelengths of light (e.g., at the red and blue end of the spectrum), the melatopes (optic axes) for each wavelength will emerge at a different point in a conoscopic field of view. This is a consequence of the dispersion curves (i.e., a plot of the three refractive indices vs. wavelength) having different slopes.

If the dispersion is pronounced, it can be recognized by red or blue color fringes appearing near the melatope and alongside the isogyres, representing different paths (and hence optic angles) for these colors of light (Fig. 22). The trick here is to understand that (i) a melatope is a point

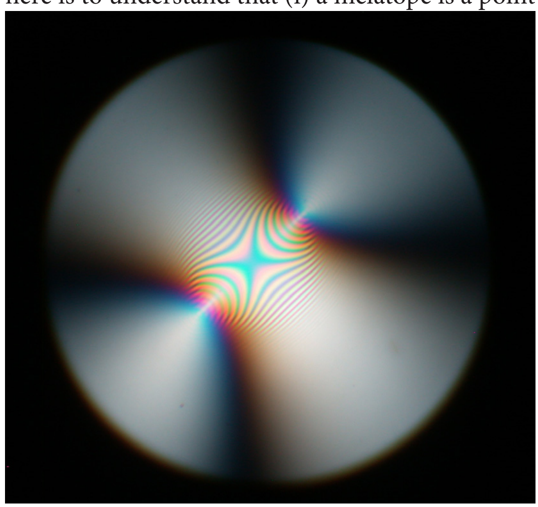

Fig. 22. A centered Bxa figure for cerussite showing strong dispersion of the optic axes; the blue fringes on the outside of the melatopes and isogyres indicate a dispersion of *r* > *v*. The high birefringence of this mineral results in a myriad of isochromes surrounding the melatopes, which quickly fade to indistinguishable high-order interference colors; they are clearly discernible, however, in monochromatic light.

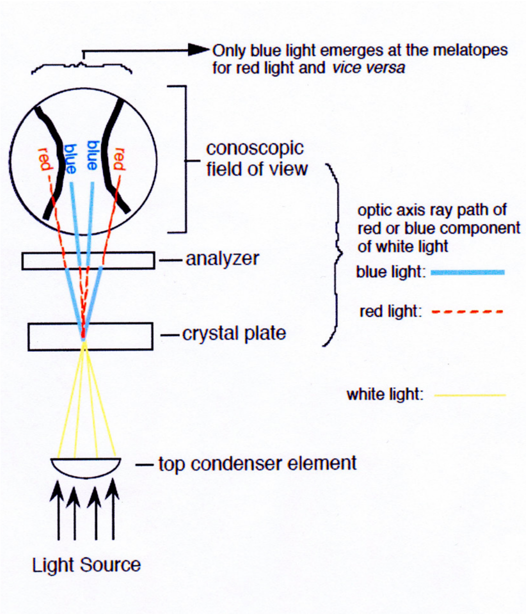

Fig. 23. Diagram showing the transmission of white light through the microscope condenser, crystal plate, and analyser, showing the ray paths for the red and blue components of white light to form a conoscopic image; note that the ray path of blue light, traveling along an isotropic direction of the optic axis, is eliminated at the analyser, leaving a red fringe that passes through to the outside of the optic axis melatope (at the concave side of the isogyre). For clarity, the biaxial Bxa hyperbolas are shown in a horizontal (E-W) position; dispersion is normally observed with the isogyres in the 45° position. Objective and Bertrand lenses are not shown for simplicity.

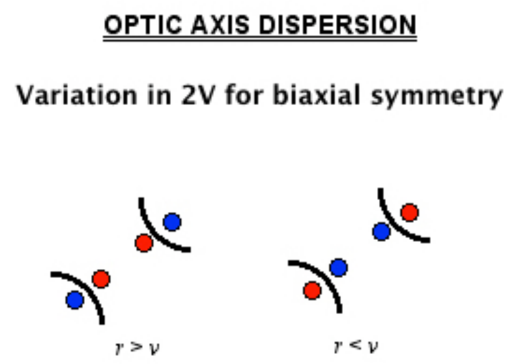

Fig. 24. A dispersion diagram for a biaxial Bxa figure showing the position of the red and blue fringes on either side of the melatope for the optic axes, for both ***r*** **>** ***v*** **and** ***r*** **<** ***v*****.**

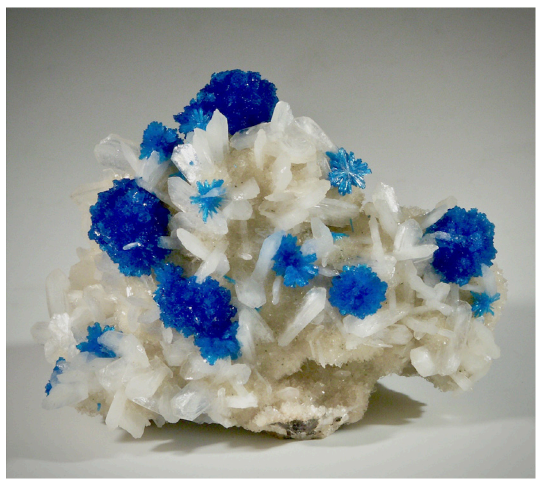

Fig. 25. A crystal specimen of cavansite on stilbite, 8 cm; from the Pune district, India.

of zero retardation, and (ii) consequently, red light traveling along an optic axis does not pass through the microscope analyser (because it experiences zero retardation), leaving only the blue color to pass through and form the interference figure. Conversely, blue light traveling along an optic axis will leave only a red fringe at the melatope. Thus, although a red fringe near the central concave (outer) part of the curved isogyre suggests that the optic angle for red light is greater than for blue light, in fact the opposite is true (Fig. 23). Accordingly, an outside red fringe would indicate that the optic angle for blue light is greater than that for red light, and is expressed as $r < v$. Conversely, a blue fringe on the outside of the melatope (as is the case for the cerussite illustrated above) indicates that the optic angle for red light is larger than that of blue light, and is expressed as $r > v$ (Fig. 24). Optic axis dispersion is further characterized as being weak, strong, very strong, or extreme, depending on the relative intensity of the color fringes.

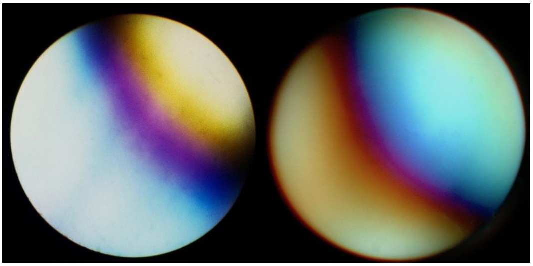

Fig. 26. A cavansite biaxial centered optic axis figure in white light (left), showing extreme optic axis dispersion, r < v (there is no waveplate in the field!). At the right is an optic axis figure for the polymorph pentagonite, which shows the reverse OA dispersion, *r > v*.

A naturally occurring mineral showing extreme optic axis dispersion is cavansite, a calcium-vanadium silicate (Fig. 25). This is a colorful blue mineral associated with zeolites from India, which appeared on the mineral market in the 1980s. The dispersion is so strong that a centered optic axis interference figure appears as if a 1 λ waveplate had been inserted (Fig. 26). Shortly thereafter, pentagonite, a polymorph of cavansite, appeared on the market. Being much more rare, these specimens commanded significantly higher prices. However, like cavansite, they also appeared as bright blue radiating crystal clusters. Differentiating the two was largely by trial and error, based only on the somewhat ambiguously elongated habit of pentagonite. It can be presumed that many misidentified cavansite specimens were sold as pentagonite at a vastly improved price. Discriminating the two is, however, very simple, requiring only a grain mount preparation and observation of a centered optic axis figure. Pentagonite is biaxial negative and shows an optic axis dispersion of $r > v$, strong (Fig. 26 right), whereas cavansite is biaxial positive and shows $r < v$, extreme (Fig. 26 left). Other minerals exhibiting this phenomenon include titanite, $r > v$, very strong, and epidote, $r > v$ strong.

Fig. 27. A single orthorhombic crystal of zoned brookite, 3.5 cm; Baluchistan, Pakistan.

Crossed Axial Plane Dispersion: Brookite.

Brookite is an orthorhombic mineral (titanium dioxide, Fig. 27) that exhibits extreme crossed axial plane dispersion. Understanding crossed axial plane dispersion for this mineral, and its relation to the wavelength (i.e., color) of light and crystal structure, further augments comprehension of the relation between mineral optics and crystal symmetry. This dispersion is often illustrated in textbooks, but usually in black and white images that can be difficult to interpret.

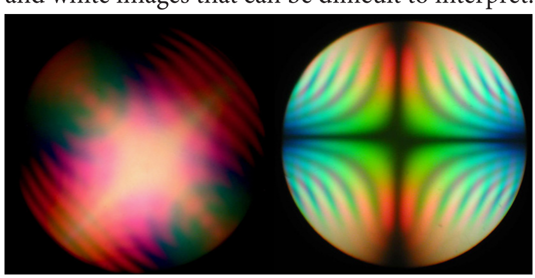

Fig. 28. Left, Bxa interference figure of brookite in the diagonal position in white light. Right, a Bxa figure in the normal (horizontal) position.

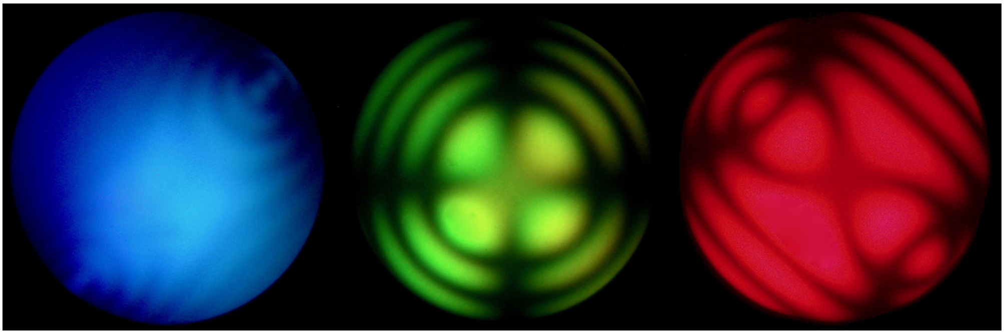

Fig. 29. Interference figures of brookite in monochromatic light: Left = Bxa figure in blue light (ca. 460 λ), center = centered optic axis figure in green light (555 λ), right = Bxa figure in red light (ca. 660 λ). The interference figure transitions from a biaxial optic plane in the NE-SW quadrants, to uniaxial in green light, to biaxial with an optic plane in the opposite NW-SE quadrants.

Crossed axial plane dispersion in brookite results in a conoscopic interference figure that, in white light, is indecipherable due to its extreme dispersion (Fig. 28). However, in monochromatic light, a normal interference figure is easily recognized. Examination with a continuous (or variable) interference filter, such as the Leitz Veril filter, shows a dynamic migration of the Biaxial Bxa isogyres as the filter is laterally moved across the light port of the microscope, from a NE-SW orientation in the blue light spectrum, to a centered uniaxial cross in green light, to a biaxial figure in the NW-SE quadrants in red light (Fig. 29). This behavior results because the dispersion curves for α (the low index of refraction) and β (the intermediate index of refraction) cross at 550 nm; at that point the crystal becomes optically uniaxial (Fig. 30). However, when the two lines cross, the high and low index of refraction are reversed, i.e., α (the *X* vibration direction)

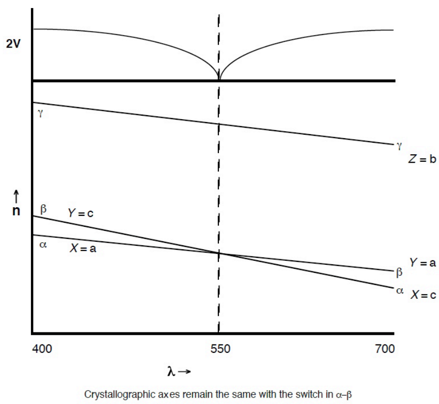

Fig. 30. A graph showing dispersion curves for the α, β and γ refractive indices (i.e. high, intermediate, and low indices) vs. wavelength. The point of crossover of the α and β lines represents a uniaxial character, with only one optic axis (note that 2V = 0 in the curve at top). On either side of this point the α and β lines are switched, however, the crystallographic axes, *a* and *c*, by definition, are not. Thus, the orientation of the Bxa figure changes with the wavelength.

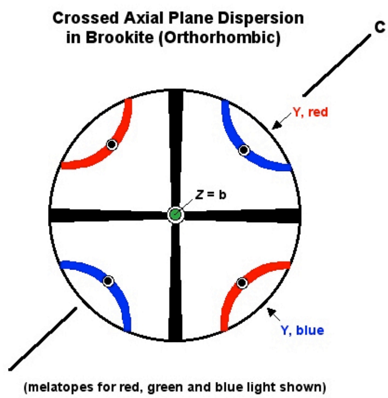

Fig. 31. Another representation of the change in the orientation of the Bxa figure (isogyres shown in the diagonal position) with wavelength in monochromatic light. During transition from blue to red light the melatopes (optic axes) migrate from a NE-SW orientation to NW-SE.

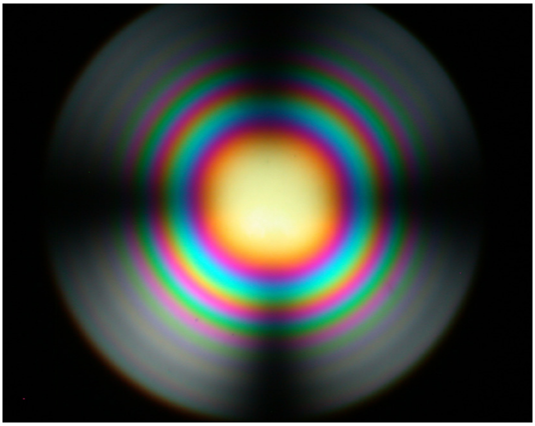

Fig. 32. A quartz interference figure from a thick crystal plate cut perpendicular to the *c*-axis, showing isochromes but an absence of isogyres in the center due to circular polarisation (optical activity) effects.

becomes β (the *Y* vibration direction) and vice versa. Thus, the optic plane (the *X-Z* plane by definition) changes with wavelength but the crystal lattice structure is fixed. Consequently, the *X* and *Y* optical directions change relative to the *a* and *c* crystallographic axes, and the Bxa interference figure must therefore transition from a NE-SW orientation in blue light to NW-SE orientation in red light (Fig. 31). Goethite shows even more extreme crossed axial plane dispersion than brookite, but the uniaxial interference figure

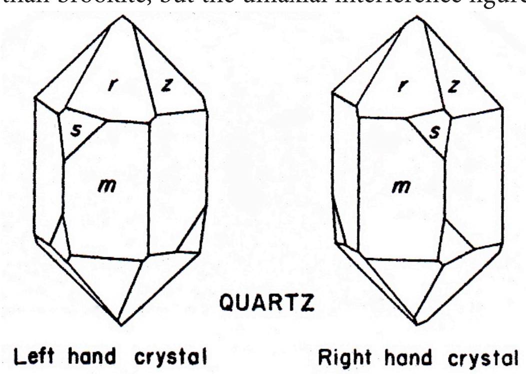

Fig. 33. A diagram of a left- and right-handed quartz crystal showing the position of the *s* face that can identify the handedness. Rhombohedral faces comprising the termination are designated as *r* (positive rhombohedral faces) and *z* (negative rhombohedral faces); *m* designates prism faces.

appears at a wavelength of ca. 620 nm vs. 555 nm for brookite.

Optical Activity: Amethyst and Cinnabar.

Quartz is a mineral that shows several curious optical properties that demonstrate both polarisation and twinning effects. These properties were related by Brewster in 1819, and published in 1823. Ordinarily, for a uniaxial crystal, in looking at the interference figure down the *c*-axis one would expect to see a centered uniaxial optic

Fig. 34. An amethyst crystal specimen, 6 cm, from Kedon, Kazakhstan.

axis figure with a black cross (with the arms representing points of extinction) extending from the center of the interference figure (a melatope) to the periphery of the conoscopic field of view. However, quartz exhibits optical activity, by which the plane of polarisation rotates as it passes through the crystal section in a direction parallel to the optic axis (which coincides with the *c*-axis); thus, the center of the conoscopic image displays only an interference color without the black isogyres (Fig. 32). Brewster (1835) further discusses this

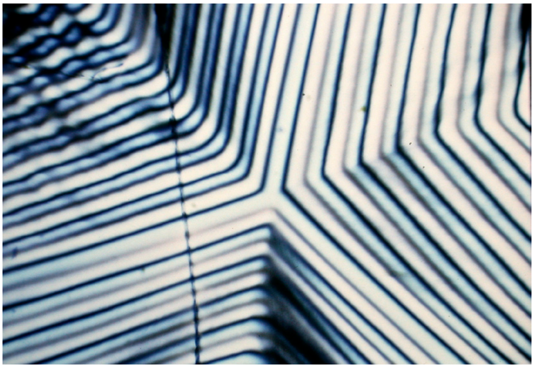

Fig. 35. A Steeg and Reuter section of amethyst cut perpendicular to the *c*-axis near the termination, showing an orthoscopic image of Brewster's fringes in crossed polarised light. The symmetrical fringes follow the rhombohedral crystallographic planes near the termination, and represent areas of zero retardation where overlapping right- and left-hand Brazil-law twins are of equal thickness.

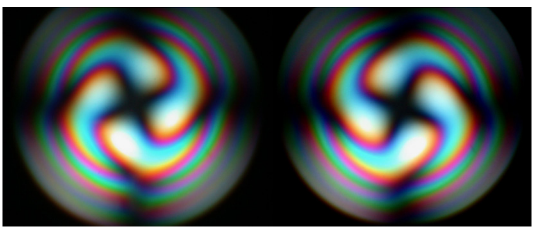

Fig. 36. Airy's spirals cut from quartz perpendicular to the *c*-axis; left shows a clockwise rotation (right-handed crystal over left), and right shows a counterclockwise rotation (left-handed crystal over right).

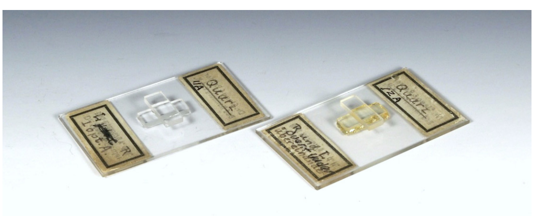

Fig. 37. Steeg & Reuter preparations of thick sections of quartz cut perpendicular to the *c*-axis, with a left-handed crystal plate superimposed on a right-handed crystal, and vice versa.

phenomenon and notes that this property (also described as circular, or rotary polarisation) was discovered by Arago in 1811. In the case of quartz, this rotation is due to the spiral silicate structure

Fig. 38. A crystal of cinnabar showing a hexagonal form, 3.5 cm; Guizhou, China. Prior to an influx of optical-grade material from China in recent years, cinnabar was extremely rare and preparations were accordingly very expensive. Unfortunately, now that cinnabar is more readily available, there are no companies remaining with the skill to prepare the mounts!

that can twist either right or left parallel to the *c*-axis; this in turn rotates the plane of polarisation either right or left, resulting in right- or left-handed crystals that can sometimes be recognized by external crystal morphology (Fig. 33).

Twinning is also common in quartz; of particular interest are the Brazil-law twins that result from a polysynthetic (i.e., repeating) intergrowth of lamellae of right- and left-handed crystals. Amethyst (Fig. 34) commonly shows this twinning in sections cut perpendicular to the *c*-axis near the rhombohedral termination, where it becomes evident under orthoscopic crossed polarised light, appearing as symmetrical dark bands following the trigonal symmetry of the pyramidal termination. These are known as Brewster's fringes (Brewster, 1823; see Fig. 35). The fringes are areas where lamellar sectors of the right- and left-handed twin crystals overlap evenly, and represent zones of zero retardation (not extinction as has been reported elsewhere). Conoscopic examination of a dark fringe yields a pattern known as an Airy's spiral. These spirals

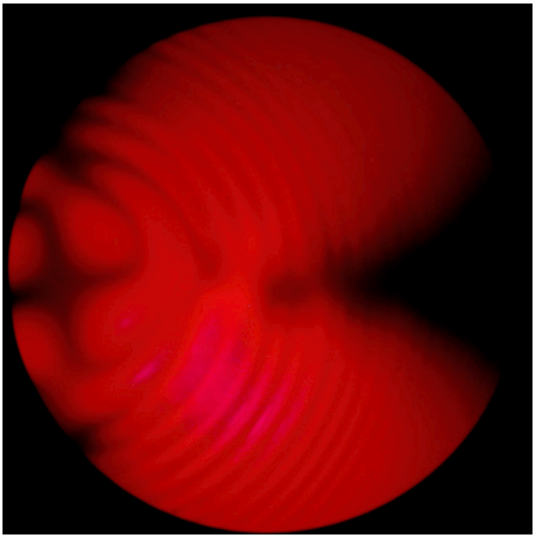

Fig. 39. An off-center optic axis figure for cinnabar in monochromatic red light, showing a CW Airy's spiral at far left.

rotate clockwise or counterclockwise, depending on whether the right-handed twin is above the left-handed twin, which yields CW rotation, or below the left-handed twin, yielding CCW rotation (Fig. 36).

The Airy's spirals can be artificially prepared if two quartz plates, right- and left-handed, both of equal thickness and cut perpendicular to the optic axes, are laid on top of each other (Fig. 37). Again, the CW or CCW direction of the spiral depends on whether a right-handed twin is placed on top of a left-handed twin, or vice versa. Brewster (1823 and 1835) and Kile (2012) provide additional information on the fascinating optical properties of quartz.

Cinnabar, a mercuric sulfide, (Fig. 38) is another of the few naturally occurring minerals with this rotary property (Fig. 39); its rotary power (per unit thickness) is ca. 15 times that of quartz. Because of its rarity and the difficulty in preparing the crystal plates, cinnabar was among the most expensive of the mounts fabricated by the firm of Steeg & Reuter; they were offered in the early

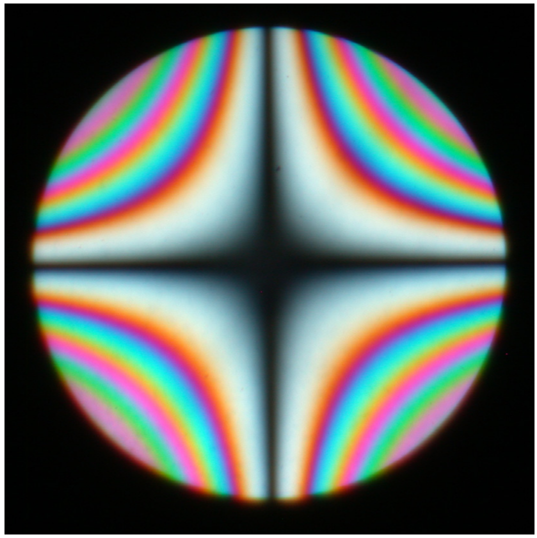

Fig. 40. Conoscopic image of crossed optic normal quartz plates cut parallel to their *c*-axes and superimposed with the *c*-axes oriented mutually perpendicular, showing the isochromes as hyperbola. This rotating compensator functions much like a Berek compensator, but without the need for a calibration table.

1900s for as much as 200 Marks, a substantial amount considering that a high-end petrographic microscope in that era cost 800 Marks.

Birefringence Hyperbola: Crossed quartz optic normal plates.

Crossing two plates of quartz that are cut *parallel* to the *c*-axis (i.e., each yielding a conoscopic optic normal, or flash figure) and cementing them at 90° (i.e., with their *c*-axes mutually perpendicular) will conoscopically yield sectored hyperbola showing the Michel-Lévy interference colors in white light (Fig. 40). This arrangement was utilized by the firm of Carl Zeiss to manufacture an instrument (the Ehringhaus compensator) for the quantitative measurement of birefringence, much like the Ernst Leitz Berek compensator (Fig. 41; see also Kile, 2023). The hyperbola in the Zeiss instrument function in an identical manner to the circular isochromes surrounding the melatope of a calcite

Fig. 41. A Carl Zeiss Ehringhaus compensator showing two graduated drums for precisely measuring the amount of tilt of the quartz plate, from which birefringence can be determined.

crystal cut perpendicular to the *c*-axis, as is found in the Berek compensator. For either compensator, tilting the crystal plate will sequentially increase the retardation (i.e., interference colours) and compensation of a grain on the microscope stage. Unlike the Berek, however, which requires calibration for each calcite plate (cut to a thickness of 0.010 mm), the Ehringhaus, on account of its much lower birefringence, can be accurately cut

Fig. 42. A tetragonal apophyllite crystal on stilbite, 9 cm, from Jalgaon, India.

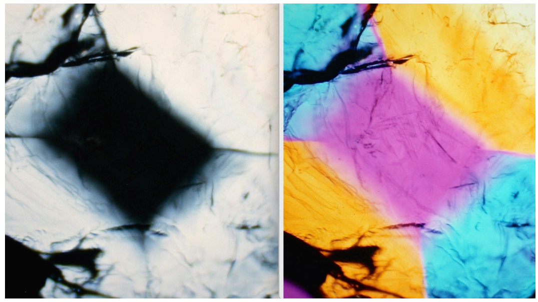

Fig. 43. Orthoscopic images of a "tessellated" apophyllite, in crossed polarised light; left = crossed polarised light, right = crossed polarised light + a 1λ waveplate. The alternating blue and yellow sectors are a result of the optic plane of the Bxa rotating 90°. These areas will show an anomalous Bxa interference figure. The central diamond-shaped core, showing a sensitive tint violet interference color, is an area of isotropic character, and will show a uniaxial cross in conoscopic illumination.

to a much thicker dimension to yield the same number of isochromes (i.e., retardation), thereby negating the need for calibration (Kile, 2003).

Mimetic Twinning, Anomalous Interference Colors: Apophyllite.

Apophyllite (or more precisely, fluorapophyllite; apophyllite is the earlier, generic term that is retained here) shows several unique properties that reinforce an understanding of a number of important optical principles, including anomalous dispersion and the relation between chemistry, crystal lattice, and optical orientation. These phenomena were first related by Brewster in 1817, and published in 1821.

Apophyllite is a prismatic mineral that crystallizes in the tetragonal system, and is usually elongated along the *c*-axis (Fig. 42). It also has perfect cleavage perpendicular to the *c*-axis. Accordingly, the expected image of a cleavage fragment under orthoscopic observation (parallel light and low magnification) should show an isotropic character

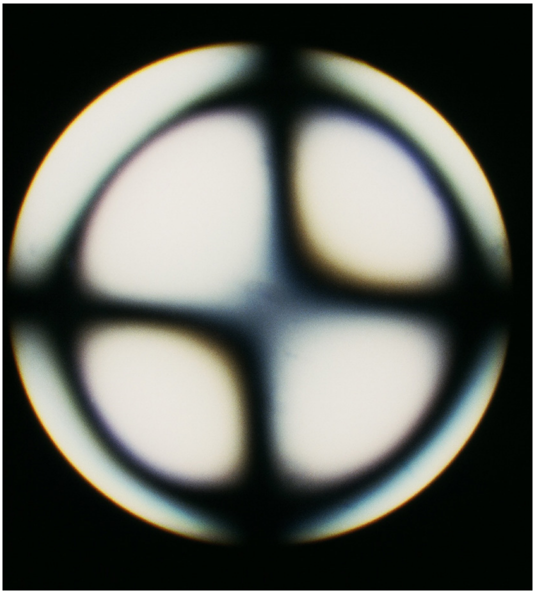

Fig. 44. A conoscopic image of an apophyllite crystal cut perpendicular to the *c*-axis [parallel to the (001) cleavage]. The tetragonal symmetry should show a uniaxial cross; instead, a biaxial Bxa figure is observed with anomalous dispersion colors (i.e., normal interference colors from the Newton scale do not appear).

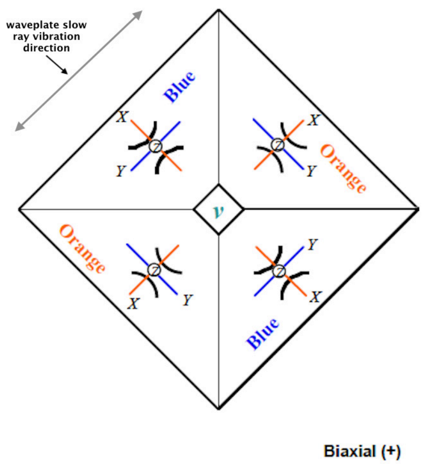

Fig. 45. A diagram of the optical orientation in an apophyllite cleavage, showing a 90° rotation of the optic plane in each of the four sectors that is caused by mimetic twinning. The rotation changes the relation of the fast (α, or *X* vibration direction) and slow (β, or *Y* vibration direction) rays in each sector relative to the γ (slow) direction in a superimposed 1λ waveplate, resulting in alternating subtractive and additive colors in the sectors seen in Fig. 43 right.

(no double refraction), whereas the conoscopic image (convergent light and high magnification) should show a uniaxial cross and a positive optic sign. However, this mineral orthoscopically shows a central isotropic core of varying size that is surrounded by four symmetrical anisotropic sectors, the pattern being described by Brewster (1821), as "tessellated" (Fig. 43, left). Notably, the pattern of tessellation changes with the depth of the cleavage fragment along the crystal prism (Brewster, 1821). Interestingly, insertion of a **1λ** waveplate onto an orthoscopic image yields subtractive colors (i.e. destructive interference, or second-order yellow-orange) in the NE-SW quadrants alternating with additive (constructive interference, or second-order blue) colors in the NW-SE quadrants (Fig. 43, right), which surround a violet central core.

Conoscopic observation furthermore shows anomalous interference colors exhibiting black isochromes against a white background (normal Michel-Lévy interference colors are absent), and an anomalous biaxial character in each of the four birefringent sectored areas (Fig. 44). Anomalous interference colors are those not found on the Newton scale; they result when birefringence and retardation are substantially different for different wavelengths of light. In contrast, this relation is the same for all wavelengths for minerals that show normal interference colors as are found on the Newton scale.

Conoscopic examination of the four sectors in the apophyllite cleavage also shows that the orientation of the acute bisectrix, or Bxa, rotates 90° in each sector. *Orthoscopic* examination of a cleavage section with a superimposed 1λ waveplate (which normally has its slow vibration direction at 45° in a NE-SW direction) confirms

Fig. 46. A monoclinic diopside crystal, 2.5 cm, from DeKalb, New York.

the changing orientation, with first-order orange in the NE and SW sectors, and first-order blue in the NW and SE sectors (Fig. 45). The central area shows a sensitive (violet) tint and represents a zone of isotropic character, which accordingly shows a conoscopic uniaxial cross. The interference color in each sector depends on whether the *X* (fast) or *Y* (slow) vibration direction of the Bxa is parallel to the slow (γ) vibration direction of the 1λ waveplate, giving either a destructive or constructive interference color (note that the slowest vibration direction, *Z*, in a biaxial positive mineral is perpendicular to the stage).

The tessellated pattern is not a feature of crystal twinning, but rather is explained by "mimetic" twinning, which is caused by the substitution of Al^{+3} into the Si^{+4} tetrahedral sites of the apophyllite, the formula of which is $KCa_4Si_8O_{20}(F,OH)\cdot 8H_2O$. The resulting distortion

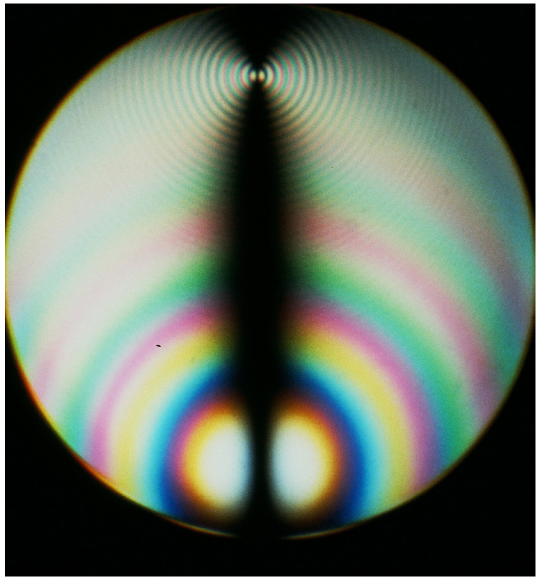

Fig. 47. At first look this appears to be a Bxa figure, but the isochromes of the two optic axes show different birefringences, which is physically impossible in a single crystal. In fact, it results from a cleverly oriented section (by Steeg & Reuter) of a twinned crystal; see accompanying diagram (Fig.48).

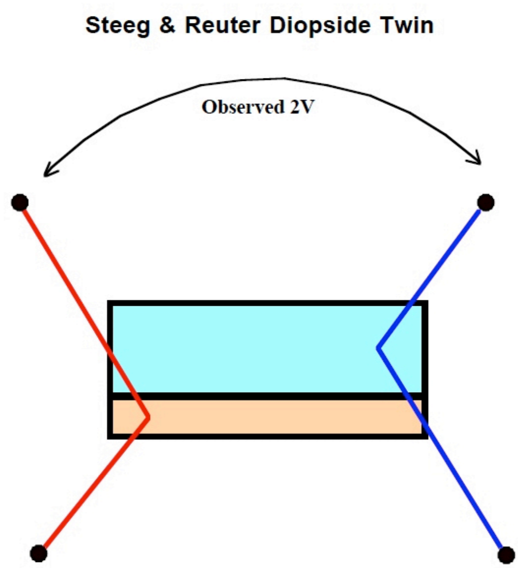

Fig. 48. Diagram of a diopside twin, with one twin superimposed over the other, and both of different thicknesses. The plate is carefully oriented to show only one optic axis from each twin, each with a different birefringence.

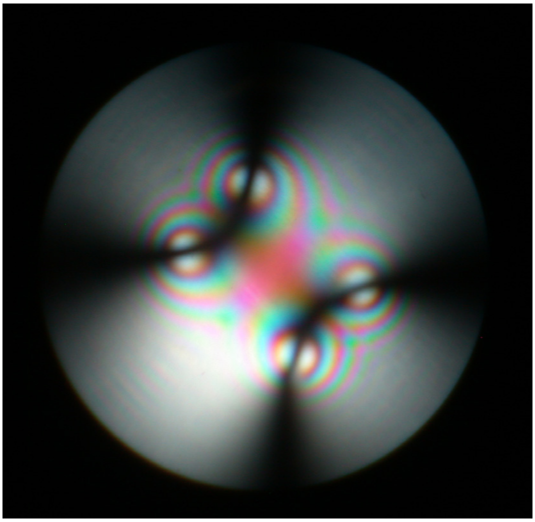

49. An aragonite acute bisectrix figure (Bxa). Viewed across a twin boundary, the Bxa (and optic axes) can be simultaneously seen from both crystals. Students are shown this figure and left to ponder what might be the cause.

of the crystal lattice leads to an anomalous biaxial character. Shtukenberg and Punin (2007) describe and explain a wide variety of synthetic organic compounds that show similar mimetic twinning phenomenon.

Peculiar and Perplexing Interference Figures: Diopside and Aragonite.

Sections through or across a twin plane can show unusual interference figures that may be difficult to interpret. It is not unusual to encounter such figures in grain mounts or in thin section preparations. The preparations described below were shown to students without explanation, and intended to get them postulating what might explain the atypical optical phenomena.

Diopside. Diopside is a biaxial clinopyroxene that often twins on the {100} or {001} crystallographic plane (Fig. 46). The image in Fig. 47 shows a biaxial mineral (diopside, a calcic clinopyroxene) with different birefringences surrounding two optic axes, but the birefringence in a given mineral should be constant unless there is a change in composition. The explanation for this unusual interference figure lies in a twinned crystal with each twin of unequal thickness and one lying on top of the other in a horizontal plane (Fig. 48). The sections were perfectly oriented by the Steeg and Reuter firm to show one optic axis contributed by each of the twinned crystals in the composite interference figure. Thus, light passing through the thinner of the superimposed plates will show a lesser birefringence and consequently fewer isochromes surrounding the optic axis, whereas light passing through the thicker crystal will show numerous isochromes surrounding the optic axis.

Aragonite. Is a tetra-axial mineral possible? Only if one inadvertently lands on the junction between a twin plane of a crystal. Aragonite (an orthorhombic calcium carbonate) is commonly twinned on {010}, which produces cyclic twins that are macroscopically visible in basal sections. Viewing a twin conoscopically at the twin boundary will yield four optic axes, with two contributed from each twin. A similar interference figure pattern is demonstrated by mica plates crossed at 60°. These are known as Reusch plates, mounts of which are seen at the upper right in Fig. 1. Peculiar interference figures are also commonly seen in thin sections of calcite, which often forms lamellar twins.

DIY (Do-It-Yourself) Preparations

Most of the preparations discussed above are rare to extremely rare, and accordingly difficult to almost impossible to obtain. However, some of them can easily be fabricated. One often needs to frequent mineral shows or browse the Internet to acquire some of the mineral samples described below.

It is the author's opinion that a grain mount preparation is the most direct and efficient means with which one can learn to recognize the various optical properties, and to ferret out an appropriate grain, based on extinction and birefringence, to measure a particular optical property. They are easily prepared via grinding and sieving from 140 to 200 mesh.

Grains are sprinkled on a glass slide with added balsam and coverslip; the refractive index of balsam is ca. 1.538, which is preferred for mineralogical preparations in that its refractive index divides two of the most common feldspar groups, plagioclase and potassium feldspar. I have mounted over 400 mineral species in grain mounts, and have learned considerably from them. Many oriented sections can be prepared if one has access to a faceting machine and a mineralogy textbook showing external crystal form vs. optical orientation diagrams (e.g. Nesse, 2013). For example, preparing crossed optic normal (ON) plates of quartz, which does not have good cleavage, requires a faceting machine to cut and polish a slice parallel to the *c*-axis (the crossed plates also need to be of equal thickness).

On the other hand, knowledge of the physical properties of minerals and crystal orientation can facilitate the preparation of useful interference figures from cleavage fragments. For example, a topaz cleavage on (001) gives a centered Bxa figure (with a 2V of ca. 60°, the melatopes are usually just outside the field of view for an objective of 0.65 NA, and just inside with a 0.85 NA objective). Another example is gypsum, where (010) cleavage fragments show an optic normal (flash) figure. An irregular cleavage will also produce numerous interference colors that can be highly artistic under low magnification (e.g., Fig. 15). Mica (muscovite) cleavages on (001) show a centered Bxa figure with a 2V of ca. 45°. Anhydrite has three cleavages ranging from good to perfect; the (001) will show a centered Bxa figure with a 2V of 44°; the cleavage on (100) will show an optic normal (or flash) figure, and the cleavage along (010) will show a Bxo (obtuse bisectrix) figure. The examples below are organized by general optical properties.

i. Anomalous twinning and interference colors.

Apophyllite shows perfect cleavage perpendicular to the *c*-axis; prismatic crystals can be cleaved with a razor blade (a light rap with small hammer will suffice). The pattern of tessellation varies along the length of the crystal. Single crystals from India are often found at mineral shows.

ii. Crossed axial dispersion.

Brookite crystals from Russia have appeared in recent years, and crystal fragments may be available (terminated crystals can be expensive); fortuitously, the Bxa is oriented perpendicular to the dominant crystal face. Micro-crystals of goethite, if transparent, provide a very similar dispersion, but with a different wavelength for the uniaxial cross. Small transparent blades can sometimes be obtained from mineral specimens.

iii. Optic axis dispersion.

Small radiating crystal groups of cavansite are readily found on the mineral market. Grain mounts will yield optic axis interference figures (look for grains with minimum birefringence). The optic axis dispersion, $r < v$, is extreme. Other minerals showing optic axis dispersion include titanite ($r > v$, very strong), epidote ($r > v$, strong), and clinozoisite ($r < v$, strong). Epidote forms a compositional series with clinozoisite, with epidote the Ca-Fe end member, and clinozoisite the Ca-Al end member. Although similar in physical appearance, they can be differentiated by their optic axis dispersion; clinozoisite is $v > r$, whereas epidote is $r > v$. Sucrose can easily be grown from aqueous solution, and many of the crystal plates fortuitously are flattened with a centered optic axis perpendicular to the crystal plane, showing a strong $v > r$ dispersion. In fact, any grain from the kitchen sugar bowl, prepared as a grain mount, will provide a nicely centered optic axis figure.

iv. Crossed mica.

The principal vibration directions of the cleavage sections need to be oriented *perfectly* at 90° and of *exactly* the same thickness (birefringence). I was able to manage four crossed plates with acceptable results, at which point I conceded further attempts, recognizing that the skill required to precisely manage additional plates is rather daunting.

v. Pleochroism.

Polished cubes of iolite have been available at mineral shows in past years, and may occasionally still appear. They provide excellent examples of strong pleochroism (e.g., Fig. 8).

Conclusions

If nothing else, optical mineralogy is colourful, and that is one element that can draw students into the realm of light, crystal structure, and chemistry. Teaching preparations not only engage the student, they also serve as a visual benchmark for recalling important optical principles. There have been many more such preparations that have been manufactured over the years than could possibly be illustrated in this article, and the reader is encouraged to pursue some of these avenues of study. Lastly, a hidden objective in writing this article is to promote the continued appreciation of optical mineralogy and the utility of the petrographic microscope that is associated with its study. No other instrument can duplicate the incredibly wide range of optical properties that can be observed and measured as does the petrographic microscope! Regrettably, at the university level this endeavor has become a dying art.

Acknowledgements

Special thanks go to Olaf Medenbach, Bochum, Germany, a mentor and friend who introduced me to many of these materials for demonstration. The author also thanks John Delly, who has steadfastly encouraged my various writing and teaching pursuits in crystal optics. John Delly, Dianne Kile, and Olaf Medenbach provided careful reviews of the manuscript.

References

Brewster, D. (1821). Account of a remarkable structure in apophyllite with observations on the optical properties of that mineral. *The Transactions of the Royal Society of Edinburgh*, v. 9, pp. 317– 336 + plates XX and XXI.

Brewster, D. (1823). On circular polarization, as exhibited in the optical structure of the amethyst, with remarks on the distribution of the colouring matter in that mineral. *The Transactions of the Royal Society of Edinburgh*, v. 9, pp. 132 – 152 + plate X.

Brewster (1835). *Treatise on Optics*. Carey, Lea, and Blanchard, Philadelphia, 323 pp. + appendix.

Delly, J.G. (2017). *Essentials of Polarized Light Microscopy and Ancillary Techniques*. Hooke College of Applied Sciences, Westmont, Illinois, 601 pp.

Fletcher, L. (1892). *The Optical Indicatrix and the Transmission of Light in Crystals*. Henry Frowde, London, 112 pp.

Kile, D.E. (2003). *The Petrographic Microscope: Evolution of a Mineralogical Research Instrument*. Special Publication No. 1, The Mineralogical Record, Tucson, Arizona, 96 pp.

Kile, D.E. (2012). Historic oriented crystal preparations by the firm of Steeg & Reuter. *Program Notes, Rochester Mineralogical Symposium/Rochester Academy of Sciences 39th Annual Meeting*, Rochester, New York, pp. 42-49.

Kile, D.E. (2012). A brief overview of the mineralogy and curious optical properties of amethyst. In *Amethyst*, Lithographie, Denver, Colorado, pp. 14-21.

Kile, D.E. (2021). Calibration and use of the Leitz Berek compensator. *Quekett Journal of Microscopy*, v. 44, pp. 91-105.

Kristjansson, L. (2003). A little known history of Helgustadir: Type locality of Iceland spar. *Matrix*, v. 93, pp. 95-107.

Medenbach, O., and Reimann, H. (2003). The Dr. Steeg & Reuter Company, Bad Homburg v.d.H., Germany – oriented crystal sections and instruments. *Journal of the Microscope Historical Society*, v. 10, pp. 100-113.

Nesse, W.D. (2013). *Introduction to Optical Mineralogy*, 4th ed. Oxford University Press, New York, 361 pp.

Shtukenberg, A. and Punin, Y. (2007). *Optically Anomalous Crystals*, B. Kahr, editor. Springer, The Netherlands, 253 pp.

Appendix – Some Abbreviated Optical Definitions

Acute Bisectrix (Bxa). The acute bisectrix represents the smaller of the two angles between intersecting optic axes in a biaxial mineral. This angle defines the optic angle, or 2V.

Anisotropic. Crystals having more than one refractive index; a medium where light passing through is split into two mutually perpendicular rays.

Birefringence. The arithmetic difference between the high and low refractive indices in an anisotropic crystal.

Conoscopic. Observation using converging light, used to examine interference figures under high magnification.

Extinction. A condition where, in an anisotropic crystal, a principal vibration direction is parallel to an eyepiece crosshair, and the crystal is dark under crossed polars.

Indices of Refraction. A measure of the velocity of light (which is inversely proportional to refraction) passing through a mineral in a given direction. For anisotropic minerals, refractive index consists of ordinary (ω) and extraordinary (ε) rays in uniaxial minerals, and α, β and γ indices in biaxial minerals (corresponding to low, intermediate and high refractive indices, which correlate with *X*, *Y*, and *Z* vibration directions). These relations are depicted with an optical indicatrix shown in most optical mineralogy textbooks. An optical indicatrix is a 3-dimensional model showing the behavior of light traveling through a mineral in terms of refractive index. This model was developed by Fletcher in 1892.

Isochrome. Rings or bands of colors of equal retardation in accordance with the Michel-Lévy color chart that can be found in most optical mineralogy textbooks.

Isogyre. Dark bands of extinction seen in a conoscopic interference figure. They represent points where the vibration directions of the fast and slow rays are parallel to an eyepiece crosshair, or to the privileged directions of the polarizers.

Isotropic. Crystals with one refractive index; a medium where light passes through in any direction without being split into two mutually perpendicular rays.

Melatope. A point of darkness (zero retardation) in a conoscopic interference figure that corresponds with the emergence of an optic axis.

Obtuse Bisectrix (Bxo). The obtuse bisectrix represents the larger of the two angles between intersecting optic axes in a biaxial mineral. See also *Acute Bisectrix*.

Optic Normal (ON). The optic normal is the direction perpendicular to the *c*-axis in a uniaxial crystal, or to the *X-Z* plane in a biaxial crystal; the interference figure for this orientation would be the optic normal, or flash figure, where diffuse isogyres enter and exit the conoscopic field of view with minimal stage rotation. Orthoscopic grains showing this orientation can be identified by the very small stage rotation that causes to grain to go from maximum brightness to extinction.

Optic Angle (2V). The smaller of two angles between the two optic axes in a biaxial mineral.

Optic Axis (OA). An isotropic direction in an anisotropic crystal, whereby light is not split into two mutually perpendicular rays. It is a point of zero retardation, evidenced by a dark (or dark-gray) mineral grain in crossed polarized light in an orthoscopic field of view, or a point of darkness in crossed polarized light in a conoscopic field of view. There is one optic axis in a uniaxial mineral, and two in a biaxial mineral.

Orthoscopic. Observation at low magnifications with parallel light rays.

Polymorph. A compound that can crystallize in different crystal structures. Diamond (cubic) and graphite (hexagonal) forms of elemental carbon are examples.

Polytype. A type of polymorph, where the stacking sequence of similar structural units or crystal planes differs, resulting in different symmetries. Common in phyllosilicates (e.g. micas).

Principal vibration direction. A "privileged" direction of light travel in an anisotropic mineral, whereby light passing through maintains its plane of vibration. There are two principal directions in a uniaxial mineral, omega (ω, the ordinary ray) and epsilon (ε, the extraordinary ray), and three principal directions in a biaxial mineral, *X*, *Y*, and *Z*, corresponding to the indices of refraction, α (fastest velocity and lowest refractive index), β (intermediate velocity and refractive index), and γ (slowest velocity and highest refractive index).

Retardation. A measure, in nm, of the lag between the fastest and slowest of mutually perpendicular rays passing through an anisotropic material.

Zero retardation. A direction of isotropic light travel, or a condition of $\Delta = i\,\lambda$, where mutually perpendicular light rays are in phase, such that no light can pass the analyser. Although zero retardation appears as a dark area, it is *not* the same as extinction.

Daniel Kile
5176 Black Bear Run
Littleton, Colorado 80125
Centennial87@Comcast.net